

Method to determine PBL height and various layers within troposphere, as measured by a lidar system

Mariana Adam¹, Carsten Gruening¹, Jean-Philippe Putaud¹

¹European Commission, Joint Research Centre, Via E. Fermi 2749, Ispra, 21020, Italy,
mariana.adam@jrc.ec.europa.eu, carsten.gruening@jrc.ec.europa.eu, jean.putaud@jrc.ec.europa.eu

ABSTRACT

The gradient method is applied to the total recorded backscatter signal (including the background) multiplied by squared range and divided by molecular backscatter coefficient and molecular transmission terms (known). Thus, the new function has a linear dependence on squared range divided by molecular backscatter and molecular transmission terms. On a 2 dimensional plot, as a function of time and range (altitude here), for each time stamp, the intercept corresponding to the derivative of the new function is determined. The mean and the standard deviation (STD) of the intercept, calculated from the derivative of the function over the far-end region (12-15km) are computed. Next, the heights where the corresponding intercepts are outside the limits defined by mean +/- 1 STD are selected. Thus, intercepts larger than the mean + 1 STD represent regions of decreasing backscatter signal and intercepts smaller than mean - 1 STD represent regions of increasing backscatter signal. In the second step of the algorithm, the planetary boundary layer (PBL) height and the delimitations of pollution layers or clouds are determined. For the layers/clouds cases, the layers/clouds can be also quantified in terms of increasing and decreasing regions.

Comparisons with the gradient method and wavelet technique, applied to RCS will be shown during conference.

1. INTRODUCTION

PBL height is an important parameter in dispersion models (e.g. [1]). On the other hand, quantification of pollution layers helps the validation of various models to predict the dispersion of the pollutants. Clouds quantification is also important in radiative models or for clouds screening in various retrievals of passive remote sensing sensors.

PBL height and other structures can be identified by analysing the profiles of various meteorological variables (e.g. temperature), gases (e.g. water vapour mixing ratio) or particulates properties (e.g. optical properties). These profiles show sharp gradients whenever heterogeneity is encountered. Routine measurements which can provide such information include radiosonde (RS) profiling, usually twice a day. Continuous measurements by a lidar system offer a complete characterization both in time and altitude. However, usually the PBL height is mainly quantified (e.g. [2-3] and the references therein). The common approaches to determine PBL height using a lidar, implies the study of range corrected signal (RCS) from few prospective. The most common ones are: the gradient method [2], the variance method [3] and the wavelet analysis [4].

The present method implies the use of the total back-

scatter signal multiplied with squared range and divided by molecular backscatter coefficient and the molecular transmission term.

2. METHOD

The lidar equation for an elastic backscatter lidar can be written as:

$$P(r) = \frac{C}{r^2} [\beta_m(r) + \beta_p(r)] T_m^2(0, r) T_p^2(0, r) + B \quad (1)$$

where $P(r)$ is the measured backscatter signal (including the background), C is the lidar constant, $\beta_m(r)$ and $\beta_p(r)$ are molecular and particulate backscatter coefficient, $T_m^2(0, r)$ and $T_p^2(0, r)$ are the molecular and particulate two-way transmission terms and B is the constant offset (background) term. The molecular term are known (either from RS profiling or using US Standard Atmosphere profiles). Equation (1) is valid for the region of complete overlap.

We define the new independent variable x as [5].

$$x(r) = \frac{r^2}{\beta_m(r) T_m^2(0, r)} \quad (2)$$

Thus, Eq. (1) becomes:

$$Y(r) = P(r)x(r) = W_p(r) + Bx(r) \quad (3)$$

where $W_p(r)$ is the first right hand side term in Eq. (1) divided by x . Thus, the new variable $Y(r)$ is a linear function of $x(r)$. For each sliding window defined over a constant range interval Δr (which will correspond to a variable Δx interval), the intercept (Y_0) of the derivative dY/dx is determined [6].

In the next step of the algorithm, the mean and a STD of Y_0 , computed over established Y_0 values (calculated over a defined far-end region) are determined (criterion 1). Next, Y_0 values outside the interval defined by mean +/- 1 STD are selected (criterion 2). Values larger than mean + 1 STD correspond to regions of decreasing backscatter signals while values smaller than mean - 1 STD correspond to regions of increasing backscatter signal.

The next step concerns the delimitation of the layers (here, clouds) and estimation of PBL height. The criterion involved to determine PBL height is based on the assumption that PBL height is the last altitude point of the first continuous decreasing region (criterion 3). Continuity assumes that there is a selected Y_0 (criterion 1) value in every altitude bin (15m). The criterion to select a layer (criterion 4) is based on assumption

that there exists a continuous increasing region followed immediately by a continuous decreasing region.

3. RESULTS AND DISCUSSIONS

The lidar data are acquired using a Cimel Cloud and Aerosol MicroLidar (CAML), belonging to European Commission, Joint Research Centre (Institute of Environment and Sustainability, Climate Change Unit). However, the presented examples use data taken during EARLINet Reference Lidar Intercomparison 2009 (EARLI09) campaign, held in Leipzig, during May 2009 (<http://www.earli09.earlinet.eu/>). Note that minimum altitude considered is 1.5km. Thus, we consider the complete overlap above 1.5km (which might not be true but we think that this assumption does not drastically affect the algorithm). The altitude interval to compute the derivative was chosen as $\Delta r=90m$. The altitude interval chosen to determine the mean and STD for Y_0 is [12 15]km. The molecular data are provided by a RS launched at 20:55 UTC.

An example of time series of the function Y versus altitude is shown in Fig. 1. Figure 2 shows Y versus x and altitude. Figure 3 shows the time series of the intercept retrieval Y_0 , as a function of altitude. Figure 4 shows an individual profile of the intercept Y_0 (22:24 UTC). Note that the extreme values reached by Y_0 are $\sim -1.45 \cdot 10^{20}$ and $\sim 10^{20}$. As also seen in Figs. 1 and 3, the largest absolute values are obtained in the region of the cloud, present at ~ 5 km.

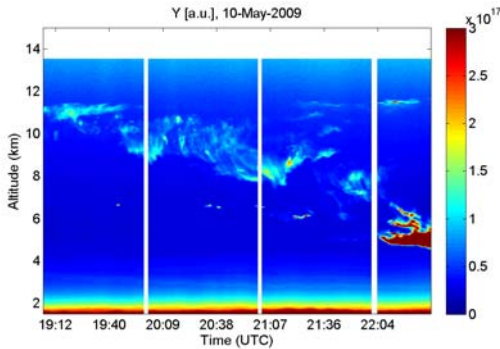


Fig. 1. Time series of Y as a function of altitude. The white strips correspond to the absence of measurements.

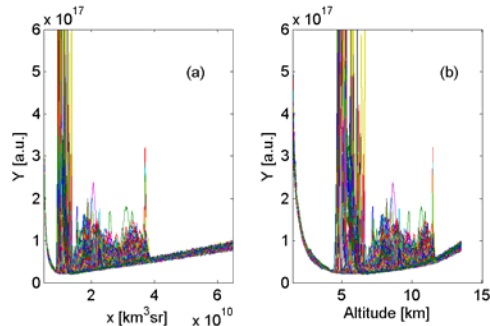


Fig. 2. Y as a function of x (a) and altitude (b). Note that in the clouds regions at ~ 5 km, Y reaches values up to $4.85 \cdot 10^{18}$ [a.u.].

The black and the red lines represent the mean and STD as determined following criterion 1.

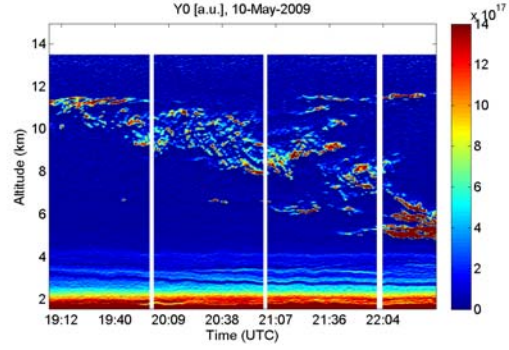


Fig. 3. Y_0 as a function of altitude.

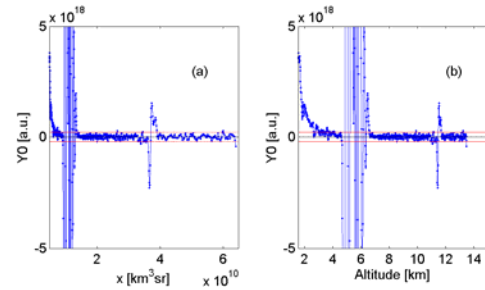


Fig. 4. Y_0 corresponding to 22:24 UTC as a function of x and altitude. The black and red lines represent the mean and STD of Y_0 calculated over the corresponding [12-15]km range. The y axis is zoomed, to emphasize the mean and STD.

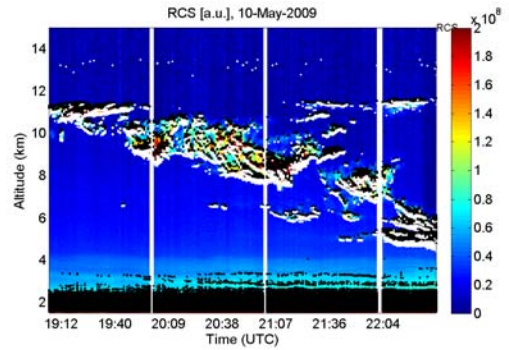


Fig. 5. RCS and the regions of sharp gradient. Black dots represent regions of decreasing RCS while white dots represent regions of increasing RCS.

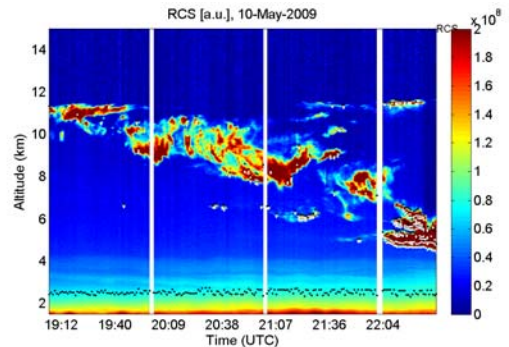


Fig. 6. RCS and overlapped PBL height and clouds delimitation.

If we overlap all the points selected using criterion 2, over a RCS plot (background subtracted), we obtain an image as shown in Fig. 5. Following criteria 3 and 4 we determine the PBL height and the clouds limits (Fig. 6). As seen in Fig. 6, the PBL height has an average value of 2.5km. However, within this time interval, PBL most likely represents the residual layer.

In Fig. 6, the increasing and decreasing regions are specified by the first and last point (thus, for each individual layer, there will be two white dots followed by two black dots).

Few discussions follow these preliminary results. As observed in Fig. 6, criterion 3 is not able to distinguish the delimitation from nocturnal boundary layer and the residual layer. However, additional criterion can be implemented taking into account that a sharp change in the intercept can be seen around 1.75km. Now, let's discuss the cloud layers. First, let's zoom over the last continuous time interval (22:04-22:33 UTC). Figure 7 shows a zoom over the [4 9]km region and a zoom over the [10 12]km region. Note that in the upper plot, the colour scale was increased, in order to emphasize the cloud structure. As can be seen, the high level cloud at 11.4km is well delimited, excepting the missing of a few time stamps. For the low level cloud, we can observe that in fact, it contains several layers. Within this time interval, the layers are quite well delimited. However, the 7-8.5km layer could not be caught.

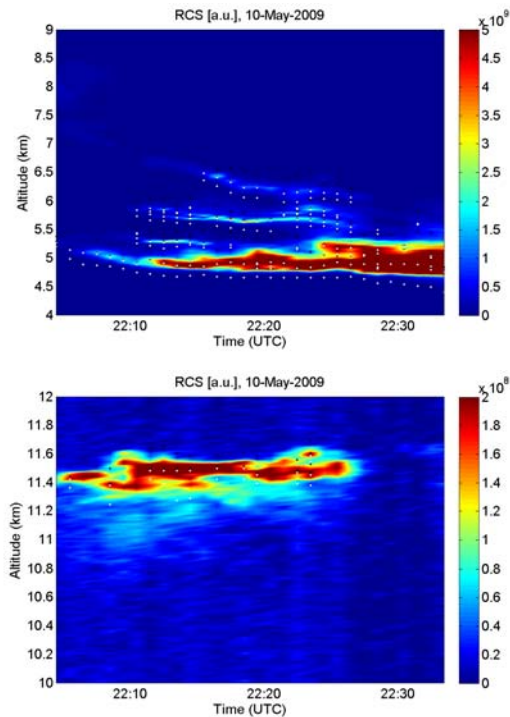


Fig. 7. Zoom over the time interval 22:04-22:33 UTC and altitude range of [4 9]km (upper plot) and [10 12]km (lower plot) respectively.

Let's now analyze the first continuous interval (19:05 – 19:59 UTC). Figure 8 shows a zoom over the altitude range of [8 12]km. As can be observed, in general, the cloud limits were not detected using the present

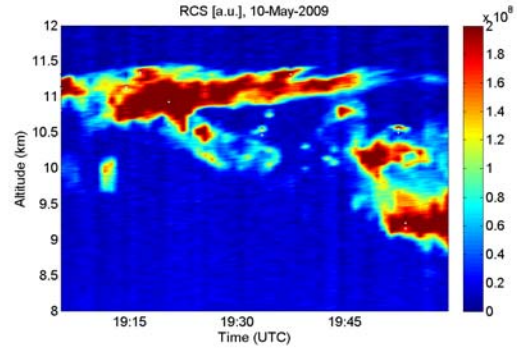


Fig. 8. Zoom over the time interval 19:05-19:59 UTC and over [8 12]km region.

criterion, based on continuity of selected negative and positive Y_0 (criterion 4). For exemplification, an individual Y_0 profile, corresponding to 19:30 UTC, is shown in Fig. 9. The altitude dependence (b) was zoomed over [9.5 12]km to emphasize the intercept points outside the mean ± 1 STD. Thus, the first negative intercept outside the inferior limit is found at ~ 9.94 km followed by another four negative intercepts until ~ 10 km. Then the first positive intercept is found at ~ 10.15 km followed by another five positive intercepts. Thus, there are nine intercept points within ± 1 STD limits which basically does not allow the continuity involved to determine a layer. Similarly, for the layer seen between ~ 11 and 11.4km (Fig. 8), there are two points inside ± 1 STD. Additional criteria are needed to encounter this situation.

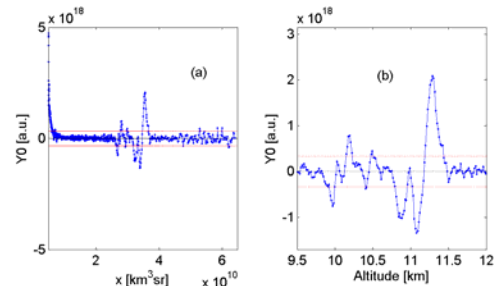


Fig. 9. Same as Fig. 4, for 19:30 UTC. The (b) plot is zoomed over the [9.5 12]km region.

4. CONCLUSIONS

The present manuscript shows preliminary results of a slightly different approach to determine PBL height and layers limits using the backscatter signal as acquired by an elastic backscatter lidar system. The first difference with respect to previous methods consists in using of the total measured backscatter signal (including the background) multiplied by squared range and divided by the molecular terms rather than using RCS (which is background subtracted). Thus, in our approach we do not subtract the offset and thus the possible errors due to a non-accurate background subtraction are eliminated. Moreover, the new defined function has a linear dependence on squared range divided by the molecular terms, which entitles us to use the derivative.

The preliminary results shown here indicate few aspects. First, the estimated PBL height most likely rep-

resents the residual layer. Secondly, the clouds delimitation is not always possible due to the restriction of criterion 4. However, additional constraints can be added in order to improve the selection of the nocturnal boundary layer (or mixed layer) on one hand and the selection of various layers on the other hand.

Note that, the present criteria (or slightly modified) can be applied to the gradient method or to the wavelet method applied to RCS (here the criteria can be applied over the wavelet details coefficients). Previous study on wavelet method was presented to BLM conference [7].

Comparisons of the current developed method with the gradient and wavelet method applied on RCS will be presented during the conference.

REFERENCES

- [1] Holstag, A. A., B. A. Boville, 1993: Local versus nonlocal boundary layer diffusion in a global climate model, *J. Climate*, **6**, 1825-1842.
 - [2] Flamant, C., J. Pelon, P. H. Flamant, P. Durand, 1997: Lidar determination of the entrainment zone thickness at the top of the unstable marine atmospheric boundary layer, *Boundary- Layer Meteorol.*, **83**, 247-284.
 - [3] Baars, H., A. Ansmann, R. Engelmann, and D. Althausen, 2008: Continuous monitoring of the boundary-layer top with lidar, *Atm. Chem. Phys.*, **8**, 7281-7296.
 - [4] Davis, K. J., N. Gamage, C. R. Hagelberg, C. Kiemle, D. H. Lenschow, and P. P. Sullivan, 2000: An objective method for deriving atmospheric structure from airborne lidar observations, *J. Atmos. Ocean. Technol.*, **17**, 1455-1468.
 - [5] Kovalev V. A., C. Wold, A. Petkov, and W. M. Hao, 2009a: Alternative method for determining the constant offset in lidar signal, *Appl. Opt.*, **48**, pp. 2559-2584.
 - [6] Kovalev V. A., A. Petkov, C. Wold, S. Urbanski, and W. M. Hao, 2009b: Determination of smoke plume and layer heights using scanning lidar data, accepted to *Appl. Opt.*
 - [7] Adam M., H. M. Calvani, and M. B. Parlange, 2004: Atmospheric boundary layer structure using wavelet analysis, *16th Symposium on Boundary Layers and Turbulence*, Portland, USA (http://ams.confex.com/ams/BLTAIRSE/techprogram/paper_80235.htm)
-